JOURNAL OF APPLIED ELECTROCHEMISTRY 23 (1993) 631–640

Generalized analytical expressions for Tafel slope, reaction order and a.c. impedance for the hydrogen evolution reaction (HER): mechanism of HER on platinum in alkaline media*

B. V. TILAK, C.-P. CHEN

Occidental Chemical Corporation, Development Center, P.O. Box 344, Niagara Falls, New York 14302, USA

Received 23 April 1992; revised 18 August 1992

Following the generally accepted mechanism of the HER involving the initial proton discharge step to form the adsorbed hydrogen intermediate, which is desorbed either chemically or electrochemically, generalized expressions for the Tafel slope, reaction order and the a.c. impedance for the hydrogen evolution reaction are derived using the steady-state approach, taking into account the forward and backward rates of the three constituent paths and the lateral interactions between the chemisorbed intermediates. Limiting relationships for the Tafel slope and the reaction order, previously published, are deduced from these general equations as special cases. These relationships, used to decipher the mechanistic aspects by examining the kinetic data for the HER on platinum in alkaline media, showed that the experimental observations can be consistently rationalized by the discharge-electrochemical desorption mechanism, the rate of the discharge step being retarded on inactive platinum compared to the same on active platinum.

Nomenclature

C_d	double-layer capacity ($\mu F\,cm^{-2}$)
E_{rev}	reversible electrode potential (V)
F	Faraday number ($96\,487\,C\,mol^{-1}$)
R	gas constant
T	temperature (K)
Y_f	Faradaic admittance ($\Omega^{-1}\,cm^{-2}$)
Y_t	Total admittance ($\Omega^{-1}\,cm^{-2}$)
Z_f	Faradaic impedance ($\Omega\,cm^2$)
i_f	total current density ($A\,cm^{-2}$)
i_{nf}	nonfaradaic current density ($A\,cm^{-2}$)
j	$\sqrt{-1}$
k_i^0	rate constant of the steps described in Equations 1 to 3 ($mol\,cm^{-2}\,s^{-1}$)
p	$j\omega$
q_{max}	saturation charge ($\mu C\,cm^{-2}$)
$\overline{\Delta i}$, $\overline{\Delta\theta}$, $\overline{\Delta E}$	Laplace transformed expressions for Δi, $\Delta\theta$ and ΔE
β_1, β_3	symmetry factors for the Equations 1 and 3
γ	saturation value of adsorbed intermediates ($mol\,cm^{-2}$)
η	overpotential
θ	coverage by adsorbed intermediates
ω	angular frequency

1. Introduction

One of the most extensively studied electrochemical reactions is the hydrogen evolution reaction (HER) in view of the perception of the simplicity of the reaction and its direct industrial relevance in water electrolysis and chlor-alkali operations. Hydrogen evolution is generally accepted to proceed via the steps (Equations 1 to 3) noted below, where in the initial proton discharge to form adsorbed H (Equation 1) is followed by either the recombination of the adsorbed H to form H_2 (Equation 2) or electrochemical desorption of the adsorbed intermediate to form H_2 (Equation 3) [1–3].

$$M + H^+ + e^- \underset{k_{-1}}{\overset{k_1}{\rightleftharpoons}} MH \qquad (1)$$

$$MH + MH \underset{k_{-2}}{\overset{k_2}{\rightleftharpoons}} H_2 + 2M \qquad (2)$$

$$MH + H^+ + e^- \underset{k_{-3}}{\overset{k_3}{\rightleftharpoons}} H_2 + M \qquad (3)$$

Mechanistic studies aimed at elucidating the elementary steps involved in the HER are generally based on the determination and interpretation of kinetic parameters such as Tafel slope, reaction order, stoichiometric number, sometimes followed by an analysis of the a.c. impedance data and open-circuit potential decay transients, obtained on a given electrode material. The diagnostic relationships employed in these analysis are often deduced taking into consideration only two of the three constituent steps (Equations 1 to 3) involved in the overall reaction and assuming that the

* This paper is dedicated to Professor Brian E. Conway on the occasion of his 65th birthday, and in recognition of his outstanding contribution to electrochemistry.

0021-891X

steps prior to the rate-determining one are in quasi-equilibrium, a situation that arises if these steps, in either direction, have rate constants at least ten times more than that for the rate-controlling reaction. More often than not, the relationships used as the guidelines for interpreting the kinetic parameters are based on the limiting behaviour, i.e. when the coverage by the adsorbed intermediates is either zero or unity.

In the course of a recent examination [4] of the literature on electrocatalysis, it has become apparent that a number of evaluations of the Tafel slope, reaction order and the a.c. impedance data found in the literature are inconsistent with the mechanisms adduced in conjoint interpretation of such values. It is the purpose of this communication to develop general expressions for the Tafel slope, reaction order and a.c. impedance based on the steady-state approach with the involvement of all the kinetic steps in the HER (Equations 1 to 3) and the lateral interaction parameter between the adsorbed hydrogen intermediates. These relationships are then used to elucidate the mechanism of the HER on platinum in alkaline media, recently examined [5,6].

2. Theory

2.1. *General expression for the Tafel slope*

The material balance for the adsorbed intermediates for the reaction scheme described by Equations 1 to 3 may be written for the steady-state condition as:

$$\gamma \frac{d\theta}{dt} = 0 = V_1 - 2V_2 - V_3 \tag{4}$$

where

$$\gamma = q_{max}/F \tag{5}$$

and

$$V_1 = k_1 C_H (1-\theta) e^{\beta_1 hE} e^{-\beta_1 g\theta} - k_{-1}\theta e^{-(1-\beta_1)hE} e^{(1-\beta_1)g\theta}$$
$$= k_1 C_H e^{\beta_1 hE} e^{-\beta_1 g\theta}(Y - \theta) \tag{6}$$

$$Y = 1 - \frac{k_{-1}\theta}{k_1 C_H} e^{-hE} e^{g\theta} \tag{7}$$

$$V_2 = k_2\theta^2 e^{2g\theta} - k_{-2}(1-\theta)^2 e^{-2g\theta}$$
$$= k_2 e^{2g\theta}(\theta^2 - X) \tag{8}$$

$$X = \frac{k_{-2}}{k_2}(1-\theta)^2 e^{-4g\theta} \tag{9}$$

$$V_3 = k_3 C_H \theta e^{\beta_3 hE} e^{\beta_3 g\theta} - k_{-3}(1-\theta) e^{-(1-\beta_3)hE} e^{-(1-\beta_3)g\theta}$$
$$= k_3 C_H e^{\beta_3 hE} e^{\beta_3 g\theta}(\theta - A) \tag{10}$$

$$A = \frac{k_{-3}}{k_3 C_H}(1-\theta) e^{-hn} e^{-g\theta} \tag{11}$$

where F/RT is written as h and C_H is the concentration of the reactant H^+ ions. In equations 6 to 11, the V's refer to the reaction rates of Equations 1 to 3, the k's refer to the rate constant for the steps noted in the subscript (equal to $k_i^0 \exp(\beta_i hE_{rev})$), E to the electrode potential and β_1 and β_3 to the symmetry factors for the forward step of Reactions 1 and 3, respectively. The exponential terms in the rate equations have been written with a positive argument for the cathodic direction of the hydrogen evolution reaction for the sake of convenience. The quantity g in Equations 6 to 11 measures, in RT units, the change of the free energy of adsorption with coverage under Temkin conditions of adsorption [7].

The total faradaic current density, i, can be expressed under steady-state conditions, based on material and charge balance conditions as:

$$\frac{i}{F} = V_1 + V_3 = 2(V_2 + V_3) \tag{12}$$

The Tafel slope, b, defined by

$$b^{-1} = \left(\frac{\partial \ln i}{\partial E}\right)_{C_H} = \frac{1}{i}\left(\frac{\partial i}{\partial E}\right)_{C_H} \tag{13}$$

can be recast from Equation 12 as:

$$b^{-1} = \left[\left(\frac{\partial V_1}{\partial E}\right)_{C_H} + \left(\frac{\partial V_3}{\partial E}\right)_{C_H}\right] \Big/ (V_1 + V_3) \tag{14}$$

where

$$\left(\frac{\partial V_1}{\partial E}\right)_{C_H} = \left[\left(\frac{\partial V_1}{\partial E}\right)_\theta + \left(\frac{\partial V_1}{\partial \theta}\right)_E \left(\frac{\partial \theta}{\partial E}\right)\right]_{C_H} \tag{15}$$

$$\left(\frac{\partial V_3}{\partial E}\right)_{C_H} = \left[\left(\frac{\partial V_3}{\partial E}\right)_\theta + \left(\frac{\partial V_3}{\partial \theta}\right)_E \left(\frac{\partial \theta}{\partial E}\right)\right]_{C_H} \tag{16}$$

or

$$b^{-1} = \left\{\left[\left(\frac{\partial V_1}{\partial E}\right)_\theta + \left(\frac{\partial V_3}{\partial E}\right)_\theta\right]_{C_H} + \left[\left(\frac{\partial V_1}{\partial \theta}\right)_E + \left(\frac{\partial V_3}{\partial \theta}\right)_E\right]_{C_H}\left(\frac{\partial \theta}{\partial E}\right)_{C_H}\right\} \Big/ (V_1 + V_3) \tag{17}$$

where $(\partial\theta/\partial E)_{C_H}$, obtained from Equation 4, is given by:

$$\left(\frac{\partial \theta}{\partial E}\right)_{C_H} = \left[\frac{\left(\frac{\partial V_1}{\partial E}\right)_\theta - \left(\frac{\partial V_3}{\partial E}\right)_\theta}{2\left(\frac{\partial V_2}{\partial \theta}\right)_E + \left(\frac{\partial V_3}{\partial \theta}\right)_E - \left(\frac{\partial V_1}{\partial \theta}\right)_E}\right]_{C_H} \tag{18}$$

Substitution of Equations 15, 16 and 18 into Equation 17 results in:

$$b = (V_1 + V_3)\left\{\left[\left(\frac{\partial V_2}{\partial \theta}\right)_E + \left(\frac{\partial V_3}{\partial \theta}\right)_E\right] + \left[\left(\frac{\partial V_2}{\partial \theta}\right)_E - \left(\frac{\partial V_1}{\partial \theta}\right)_E\right]\right\}_{C_H} \Big/ 2\left\{\left(\frac{\partial V_1}{\partial E}\right)_\theta \left[\left(\frac{\partial V_2}{\partial \theta}\right)_E + \left(\frac{\partial V_3}{\partial \theta}\right)_E\right] + \left(\frac{\partial V_3}{\partial E}\right)_\theta \left[\left(\frac{\partial V_2}{\partial \theta}\right)_E - \left(\frac{\partial V_1}{\partial \theta}\right)_E\right]\right\}_{C_H} \tag{19}$$

Equation 19 is the general description of the Tafel slope for the HER proceeding via the pathways of

Equations 1 to 3. Exact expression for the discharge–recombination mechanism and discharge–electrochemical desorption mechanism can be obtained by substituting the following derivatives into Equation 19:

$$\left(\frac{\partial V_1}{\partial E}\right)_{\theta,C_H} = \frac{V_1 h[\beta_1(Y-\theta)+(1-Y)]}{Y-\theta} \quad (20)$$

$$\left(\frac{\partial V_3}{\partial E}\right)_{\theta,C_H} = \frac{V_3 h[\beta_3(\theta-A)+A]}{\theta-A} \quad (21)$$

$$\left(\frac{\partial V_1}{\partial \theta}\right)_{E,C_H} = \frac{V_1\{(Y-1-\theta)+g\theta[(Y-1)-\beta_1(Y-\theta)]\}}{\theta(Y-\theta)} \quad (22)$$

$$\left(\frac{\partial V_2}{\partial \theta}\right)_{E,C_H} = V_2(2g+M) \quad (23)$$

$$M = \frac{2\theta + \frac{2k_{-2}}{k_2}(1-\theta)e^{-4g\theta}[1+2g(1-\theta)]}{\theta^2 - X} \quad (24)$$

$$\left(\frac{\partial V_3}{\partial \theta}\right)_{E,C_H} = \frac{V_3\{g(1-\theta)[\beta_3(\theta-A)+A]+(1-\theta+A)\}}{(1-\theta)(\theta-A)} \quad (25)$$

2.1.1. Discharge–recombination. The Tafel slope for this coupled sequence can be obtained, by substituting Equations 20 to 25 into Equation 19 with $V_3 \longrightarrow 0$, as

$$b = \frac{RT}{F}\{M\theta(1-\theta)-(Y-\theta-1) + g\theta[Y-2\theta+1+\beta_1(Y-\theta)]\}/ \{M\theta[\beta_1(Y-\theta)+(1-Y)] + 2g\theta[Y(\beta_1-1)-2\beta_1\theta+2]\} \quad (26)$$

which, when $\beta_1 = 0.5$ and the first step is in quasi-equilibrium, i.e. when $Y = \theta$, degenerates to the results reported earlier [8,9], as

$$b = \frac{RT}{F}\left[\frac{1+g\theta(1-\theta)}{2(1+g\theta)(1-\theta)}\right] \quad (27)$$

When $g = 0$, it can be noted from Equation 27 that $b = RT/2F$ as $\theta \longrightarrow 0$ and $b \longrightarrow \infty$ as $\theta \longrightarrow 1$, which is a well-known result.

2.1.2. Discharge-electrochemical desorption. The Tafel slope for the sequence can be obtained from Equation 19 by substituting $V_2 = 0$ and $Y - \theta = \delta(\theta - A)$ where $\delta = (k_3/k_1)e^{g\theta}$, the resulting expression being:

$$b = \left(\frac{RT}{F}\right)\langle L\{(1-\theta)+\delta(\theta-L) + g\theta(1-\theta)[\theta(\delta-1)+1 - \delta L(2-\beta_1-\beta_3)]\}\rangle/\langle\theta(1-L) \times (1-\theta-\beta_1\delta L) - \{(1-\theta) \times [\theta-(1-\beta_3)L](\delta L-1)\} + g\theta \times \{(1-\theta)[\theta-(1-\beta_3)L][2(1-\theta)-\delta L]\}\rangle \quad (28a)$$

where $L = \theta - A$. When $k_{-3} \longrightarrow 0$ (i.e. $A \longrightarrow 0$) and $\beta_1 = \beta_3 = \beta$, the Tafel slope expression can be deduced as

$$b = \frac{RT}{F}\{1+g\theta[1-\theta(1+\delta)]/\beta[1+g\theta(1-\theta)] + (1+\beta g\theta)[1-\theta(1+\delta)]\} \quad (28b)$$

which degenerates to Equation 29 when the first step is in quasi-equilibrium.

$$b = \frac{RT}{F}\left[\frac{1+g\theta(1-\theta)}{\beta+(1-\theta)(1+g\theta)}\right] \quad (29)$$

Thus, when $\beta = 0.5$ and $\theta \longrightarrow 0$, $b = 2RT/3F$ and when $\theta \longrightarrow 1$, $b = 2RT/F$.

2.2. *General expression for the reaction order*

The reaction order for the HER can be deduced in the same manner as above by writing

$$\mathscr{R} = \left(\frac{\partial \ln i}{\partial \ln C_H}\right)_E = \frac{C_H}{V_1+V_3}\left[\left(\frac{\partial V_1}{\partial C_H}\right)_E + \left(\frac{\partial V_3}{\partial C_H}\right)_E\right] \quad (30)$$

where

$$\left(\frac{\partial V_1}{\partial C_H}\right)_E = \left[\left(\frac{\partial V_1}{\partial C_H}\right)_\theta + \left(\frac{\partial V_1}{\partial \theta}\right)_{C_H}\left(\frac{\partial \theta}{\partial C_H}\right)\right]_E \quad (31)$$

$$\left(\frac{\partial V_3}{\partial C_H}\right)_E = \left[\left(\frac{\partial V_3}{\partial C_H}\right)_\theta + \left(\frac{\partial V_3}{\partial \theta}\right)_{C_H}\left(\frac{\partial \theta}{\partial C_H}\right)\right]_E \quad (32)$$

or

$$\mathscr{R} = \frac{C_H}{V_1+V_3}\left[\left(\frac{\partial V_1}{\partial C_H}\right)_\theta + \left(\frac{\partial V_3}{\partial C_H}\right)_\theta\right]_E + \left[\left(\frac{\partial V_1}{\partial \theta}\right)_{C_H} + \left(\frac{\partial V_3}{\partial \theta}\right)_{C_H}\right]_E\left(\frac{\partial \theta}{\partial C_H}\right)_E \quad (33)$$

Substitution of $(\partial\theta/\partial C_H)_E$ expressed by

$$\left(\frac{\partial \theta}{\partial C_H}\right)_E = \left[\frac{\left(\frac{\partial V_1}{\partial C_H}\right)_\theta - \left(\frac{\partial V_3}{\partial C_H}\right)_\theta}{2\left(\frac{\partial V_2}{\partial \theta}\right)_{C_H} + \left(\frac{\partial V_3}{\partial \theta}\right)_{C_H} - \left(\frac{\partial V_1}{\partial \theta}\right)_{C_H}}\right]_E \quad (34)$$

results in a general expression for the reaction order as:

$$\mathscr{R} = \frac{2C_H}{V_1+V_3}\left\{\left(\frac{\partial V_1}{\partial C_H}\right)_\theta\left[\left(\frac{\partial V_2}{\partial \theta}\right)_{C_H} + \left(\frac{\partial V_3}{\partial \theta}\right)_{C_H}\right] + \left(\frac{\partial V_3}{\partial C_H}\right)_\theta\left[\left(\frac{\partial V_2}{\partial \theta}\right)_{C_H} - \left(\frac{\partial V_1}{\partial \theta}\right)_{C_H}\right]\right\}_E / \left\{\left[\left(\frac{\partial V_2}{\partial \theta}\right)_{C_H} + \left(\frac{\partial V_3}{\partial \theta}\right)_{C_H}\right]\right.$$

$$+\left[\left(\frac{\partial V_2}{\partial\theta}\right)_{C_H}-\left(\frac{\partial V_1}{\partial\theta}\right)_{C_H}\right]\Bigg\}_E \quad (35)$$

where

$$\left(\frac{\partial V_1}{\partial C_H}\right)_{\theta,E}=\frac{V_1(1-\theta)}{C_H(Y-\theta)} \quad (36)$$

and

$$\left(\frac{\partial V_3}{\partial C_H}\right)_{\theta,E}=\frac{V_3\theta}{C_H(\theta-A)} \quad (37)$$

2.2.1. Discharge–recombination. The reaction order for this mechanism may be obtained by substituting $V_3 = 0$ in Equation 35 as

$$\mathscr{R} = \theta(1-\theta)(2g+M)/\theta(Y-\theta)(2g+M) - (Y-\theta-1)+g\theta[\beta_1(Y-\theta)-(Y-1)] \quad (38)$$

Equation 38 can easily be degenerated to the previously known results when $\beta_1 = 0.5$ and when the first step is in quasi-equilibrium as

$$\mathscr{R}=\frac{2(1+g\theta)(1-\theta)}{1+g\theta(1-\theta)} \quad (39)$$

which shows that $\mathscr{R} = 2$ when $\theta \longrightarrow 0$ and $\mathscr{R} = 0$ as $\theta \longrightarrow 1$.

2.2.2. Discharge–electrochemical desorption. The reaction order for this mechanism can be deduced from Equation 35 by substituting $V_2 = 0$ and $Y - \theta = \delta(\theta - A)$. Again, the $\mathscr{R}$ for this mechanism is a complex function of θ and g as can be noted from Equation 40.

$$\begin{aligned}\mathscr{R} = {} & \theta(1-\theta)[(1-L)+(1-\delta L)] \\ & + g\{(1-\theta)[\theta-(1-\beta_3)L] \\ & + \theta[1-\theta-(1-\beta_1)\delta L]\}/ \\ & L\{(1-\theta)+\delta(\theta-L)+g\theta(1-\theta) \\ & \times[\theta(\delta-1)+1-\delta L(2-\beta_1-\beta_3)]\}\end{aligned} \quad (40)$$

However, when $\beta_1 = \beta_3 = \beta$ and $k_{-3} \longrightarrow 0$, $\mathscr{R}$ can be obtained as

$$\mathscr{R}=1+\frac{[1-\theta(1+\delta)](1-\beta g\theta)}{1+g\theta(1-\theta)} \quad (40)$$

which degenerates to

$$\mathscr{R}=2-\theta \quad (41)$$

when the discharge step is at quasi-equilibrium and $g = 0$.

2.3 *General expression for the a.c. impedance*

The a.c. impedance for the HER can be deduced in the same manner as above by writing

$$Z_f=\frac{1}{Y_f}=\left(\frac{\overline{\Delta i}}{\overline{\Delta E}}\right)_{C_H} \quad (42)$$

and by linearizing Equation 4 as

$$\gamma\frac{d\Delta\theta}{dt}=\Delta V_1-2\Delta V_2-\Delta V_3 \quad (43)$$

where

$$\Delta V_1=\left(\frac{\partial V_1}{\partial\theta}\right)_{E,C_H}\Delta\theta+\left(\frac{\partial V_1}{\partial E}\right)_{\theta,C_H}\Delta E \quad (44)$$

$$\Delta V_2=\left(\frac{\partial V_2}{\partial\theta}\right)_{E,C_H}\Delta\theta \quad (45)$$

$$\Delta V_3=\left(\frac{\partial V_3}{\partial\theta}\right)_{E,C_H}\Delta\theta+\left(\frac{\partial V_3}{\partial E}\right)_{\theta,C_H}\Delta E \quad (46)$$

Substituting Equations 44–46 into Equation 43, followed by Laplace transformation of Equation 43 results in

$$\left(\frac{\overline{\Delta\theta}}{\overline{\Delta E}}\right)_{C_H}=\frac{\left[\left(\frac{\partial V_1}{\partial E}\right)_\theta-\left(\frac{\partial V_3}{\partial E}\right)_\theta\right]_{C_H}}{p\gamma+\left[2\left(\frac{\partial V_2}{\partial\theta}\right)_E+\left(\frac{\partial V_3}{\partial\theta}\right)_E-\left(\frac{\partial V_1}{\partial\theta}\right)_E\right]_{C_H}} \quad (47)$$

Equation 12, in a linearized form, can be expressed as

$$\frac{\Delta i}{F}=\left[\left(\frac{\partial V_1}{\partial\theta}\right)_E+\left(\frac{\partial V_3}{\partial\theta}\right)_E\right]_{C_H}\Delta\theta+\left[\left(\frac{\partial V_1}{\partial E}\right)_\theta+\left(\frac{\partial V_3}{\partial E}\right)_\theta\right]_{C_H}\Delta E \quad (48)$$

Hence, the faradaic admittance can be obtained by taking the Laplace transformation of Equation 48 and substituting in Equation 47 as noted below.

$$\begin{aligned}Y_f &= \left(\frac{\overline{\Delta i}}{\overline{\Delta E}}\right)_{C_H} \\ &= F\left[\left(\frac{\partial V_1}{\partial\theta}\right)_E+\left(\frac{\partial V_3}{\partial\theta}\right)_E\right]_{C_H}\left(\frac{\overline{\Delta\theta}}{\overline{\Delta E}}\right)_{C_H} \\ &\quad + F\left[\left(\frac{\partial V_1}{\partial E}\right)_\theta+\left(\frac{\partial V_3}{\partial E}\right)_\theta\right]_{C_H}\end{aligned} \quad (49)$$

Since $i = i_f + i_{nf}$, the total admittance for the HER, Y_t can now be written as

$$Y_t = Y_f + pC_d \quad (50a)$$

The real and imaginary components of the impedance can be obtained [10] from Equations 42 and 50 by substituting $p = j\omega$. Complex-plane diagrams will reveal two semicircles when $(\overline{\Delta\theta}/\overline{\Delta E})_{C_H}$ is finite, and when $(\overline{\Delta\theta}/\overline{\Delta E})_{C_H} = 0$, only one semicircle, originating from C_d, is expected.

When there is coupling between the double layer charging and faradaic process, the total admittance can be derived to be, as outlined in [10]:

$$Y_t = Y_f + pC_d + p\left(\frac{\partial q_m}{\partial\theta}\right)\left(\frac{\overline{\Delta\theta}}{\overline{\Delta E}}\right)_{C_H} \quad (50b)$$

However, calculations based on Equations 49 and 50b showed negligible change in the total impedance from the additional term arising from the faradaic–nonfaradaic coupling.

3. Results and discussion

Global expressions for $\mathscr{R}$, b and Z were derived for reaction pathways such as those proposed for the HER in Section 2 using the steady-state approach without any assumption regarding the rate-determining step. These relationships, general in nature, were shown to degenerate to the previously published [1 to 3] limiting values for the slow-recombination and slow-electrochemical desorption mechanisms. The methodology employed in Section 2 is novel, unique and can be easily adopted for obtaining the b and $\mathscr{R}$ dependence on η for other electrochemical reaction pathways involved in oxygen evolution reaction, oxygen reduction reaction, etc.

3.1. *Components of Tafel slope*

An examination of Equation 17 shows that the Tafel slope, a complex function of θ and η (see Equations 17), can be separated into two components as

$$\frac{1}{b} = \frac{1}{b_1} + \frac{1}{b_2} \tag{51}$$

where

$$\frac{1}{b_1} = \frac{\left[\left(\frac{\partial V_1}{\partial E}\right)_\theta + \left(\frac{\partial V_3}{\partial E}\right)_\theta\right]_{C_H}}{V_1 + V_3} \tag{52}$$

$$\frac{1}{b_2} = \frac{\left[\left(\frac{\partial V_1}{\partial \theta}\right)_E + \left(\frac{\partial V_3}{\partial \theta}\right)_E\right]_{C_H} C_\phi}{\gamma(V_1 + V_3)} \tag{53}$$

and

$$C_\phi = \gamma\left(\frac{\partial \theta}{\partial E}\right)_{C_H} \tag{54}$$

It can easily be seen from Equation 51 that adsorbed intermediates, through the adsorption pseudocapacitance defined as $(\partial\theta/\partial E)_{C_H}$, lowers the magnitude of the Tafel value; the pseudocapacitance independent value being given by Equation 52. Substitution of Equations 6, 7, 10, 11, 20 and 21 in Equation 52 with $\beta_1 = \beta_3 = \beta$, results in an explicit expression for b_1^{-1} as

$$b_1^{-1} = \beta h + h\left[\frac{\delta A + 1 - Y}{\theta(\delta - 1) - \delta A + Y}\right] \tag{55}$$

Expressing θ, from Equations 6 and 10, as

$$\theta = \frac{k_3 A + k_1 Y}{k_1 + k_3} \tag{56}$$

and substituting it in Equation 55 results in a relationship for b_1 as

$$b_1 = \frac{RT}{F}\left[\frac{2k_1 k_3(Y - A)}{k_1^2(1 - Y) + k_3(k_3 A + k_1)}\right] \tag{57}$$

Thus, b_1 is a complex function of the coverage and the constituent rate constants of steps 1 and 3, assuming a limiting value of $RT/\beta F$ as may be noted by neglecting the backward rates for steps 1 and 3.

Deviation of the experimentally determined Tafel slope from the pseudocapacitance independent value of Tafel slope of $RT/\beta F$ is indicative of the active participation of the adsorbed intermediates in the rate-controlling pathway. Hence, consistent mechanistic evaluations should not only involve Tafel slope determination but must be complimented by the measurements of the overpotentially deposited coverage by the adsorbed intermediates, and the often neglected reaction orders. a.c. impedance measurements do provide information related to $(\partial\theta/\partial E)_{C_H}$ but are not as direct and unambiguous as the data obtained from the potential-relaxation technique as convincingly demonstrated by Conway and his coworkers [4]. The need for complimentary measurements of C_ϕ, $\mathscr{R}$ and b to arrive at a mechanism can be exemplified by considering a situation when $b = RT/\beta F$, $C_\phi \sim 0$ (based on potential-relaxation studies) and $\mathscr{R} = 2$. These values are consistent with the slow-discharge mechanism and should exhibit only one semi-circle, obvious from Equations 49 and 50, corresponding to the double-layer capacity in the Nyquist-plots on planar electrodes. However, if the impedance plot shows two semi-circles and $b = RT/\beta F$ with $(\partial\theta/\partial E)_{C_H} = 0$, then either the slow-step is not the primary discharge reaction or the measurements are questionable.

Another case of interest is the explanation of $b = 1.5RT/F$ with $(\partial\theta/\partial E)_{C_H} = 0$ during the course of the HER. Assuming the mechanism to be slow-discharge–fast-electrochemical desorption, $b = 1.5RT/F$ can be explained by proposing the β value to be 0.66. Alternately, for $\beta = 0.5$, it is possible to estimate k_3/k_1 for various θ values using Equation 58, obtained from Equation 28 for $k_{-3} \longrightarrow 0$ and $g = 0$.

$$b = \frac{RT}{F}\left[\frac{1}{1 + \beta - \theta(1 + \delta)}\right] \tag{58}$$

For $b = 1.5RT/F$, k_3/k_1 would be ~ 83 for $\theta = 0.01$ and 17 for $\theta = 0.05$. These estimates of rate constants may now be refined by iterative evaluation using Equation 28 and experimental verification.

The kinetic data for the HER on platinum in alkaline media using the relationships developed in Section 2 are now evaluated.

3.2. *Mechanism of the h.e.r. on platinum from alkaline media*

The mechanism of HER on platinum in alkaline solutions was recently examined by Conway *et al.* [11] and Bai *et al.* [5] by the potential-decay method [12, 13] complimented by steady state and a.c. impedance studies. These investigations showed (see Fig. 1) a Tafel slope value of ~ 125 mV on unactivated Pt in 0.5 M NaOH solutions which was cathodically prepolarized at an overpotential of 0.1 V for 1 h, whereas anodically activated platinum in 0.5 M NaOH solutions exhibited a Tafel slope of 75 mV in the low overpotential range and, a b value of 125 mV at overpotentials of > 0.1 V. Analysis of potential relaxation

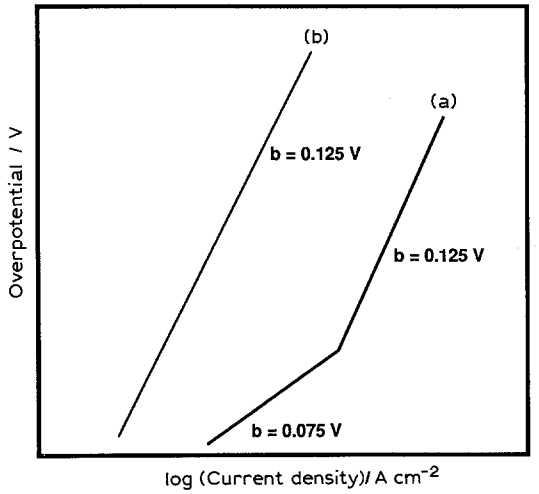

Fig. 1. Schematic polarization data for HER on active platinum (a) and inactive platinum (b) in 0.5 M NaOH (from [11]).

transients showed significant pseudocapacitance in the overpotential range of 0 to 0.1 V with activated platinum suggesting the low Tafel slope of 75 mV to be arising from the participation of adsorbed intermediates in the rate-controlling pathway. On the other hand, the coverage by adsorbed hydrogen intermediates on unactivated platinum was found to be ~ 0.1. Complex-plane impedance plots obtained with activated platinum, schematically depicted in Fig. 2, showed a broad semi-circle with a minor end at the high frequency end, at low η values; two overlapping semi-circles in the η range of 0.1 to 0.15 V and a single semicircle with a shoulder at the low frequency end at η values of >0.15 V. The impedance spectra with unactivated platinum revealed no distinct features, mostly exhibiting two unresolved overlapping semicircles in the overpotential range of 0.1 to 0.3 V.

The a.c. impedance and the Tafel slope data were explained [5, 11] in terms of initial discharge of H_2O followed by parallel recombination–electrochemical desorption mechanism, the rates of these steps being comparable. On activated platinum, the recombination step was considered to make a major contribution to the reaction rate whereas, on unactivated platinum surfaces, the discharge step was proposed to be rate-controlling. A saturation coverage value of

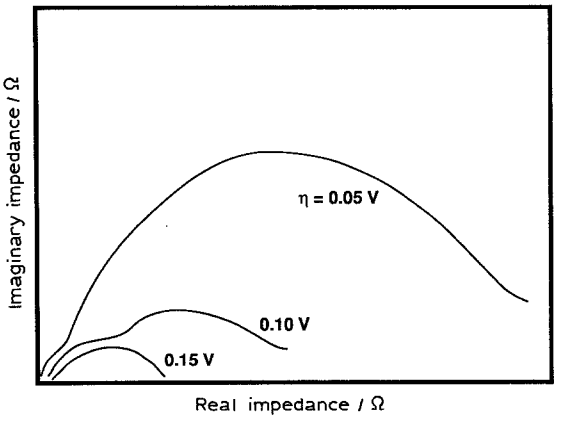

Fig. 2. Schematic Nyquist plots for HER on active platinum in 0.5 M NaOH at various overpotentials (from [5]).

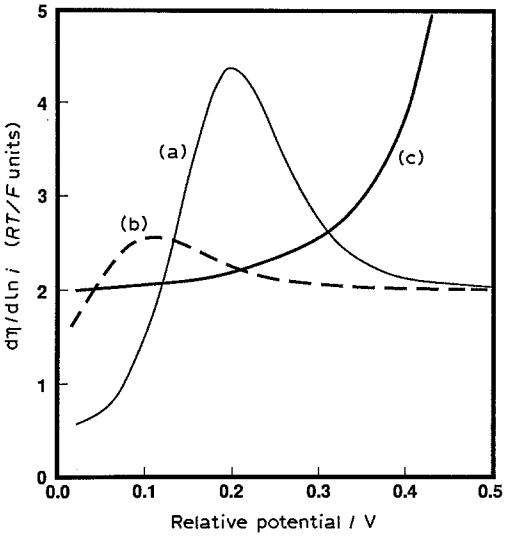

Fig. 3. Calculated Tafel slope variations with potential employing the following rate constants: (a) $k_1 = 1 \times 10^{-8}$, $k_{-1} = 3 \times 10^{-7}$, $k_2 = 2.8 \times 10^{-8}$, $k_3 = 2 \times 10^{-10}$; (b) $k_1 = 1.5 \times 10^{-10}$, $k_{-1} = 1.5 \times 10^{-10}$, $k_2 = 2.2 \times 10^{-10}$, $k_3 = 2.2 \times 10^{-11}$; (c) $k_1 = 5 \times 10^{-9}$, $k_{-1} = 2.5 \times 10^{-9}$, $k_2 = 5 \times 10^{-6}$, $k_{-2} = 2 \times 10^{-9}$. The rate constants reported in [5] and [11] are used in (a) and (b) and the k values in [6] are used in (c).

70 μC cm^{-2} was used in the calculations with activated platinum and 20 μC cm^{-2} for unactivated platinum in contrast to the generally chosen value of 210 μC cm^{-2} for unit coverage by adsorbed hydrogen.

Ekdunge *et al.* [6], examining the kinetics of HER on platinum in 1 M KOH solutions, obtained similar results to that of Conway *et al.* [5, 11] and proposed a coupled discharge–recombination mechanism. The rate constants reported by Conway *et al.* [5, 7] and Ekdunge *et al.* [6] are noted below for the HER on platinum in alkaline solutions along with other kinetic data.

It may be noted that although the platinum electrodes of Ekdunge *et al.* [6] were electrochemically activated for 10 min by polarization every second between ± 1 mA cm^{-2} and exhibited an i_0 value of 3.1×10^{-4} A cm^{-2}, similar to the activated platinum

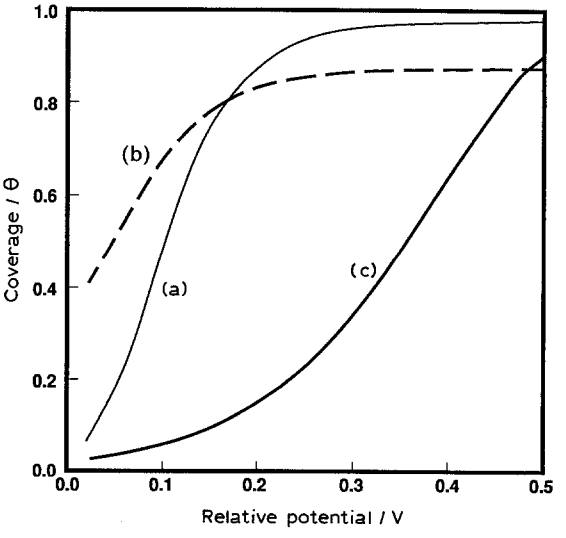

Fig. 4. Calculated coverage dependence on potential for the three cases quoted in Fig. 3 and Table.1

Table 1. Kinetic data for HER on platinum in alkaline media at 25° C

Rate constants /mol cm^{-2} s^{-1}	*Conway et al. [5, 7] Pt in 0.5 M NaOH*		*Ekdunge et al. [6] Pt in 1 M KOH**
	Active Pt	*Inactive Pt*	
k_1	1×10^{-8}	1.5×10^{-10}	5×10^{-9}
k_{-1}	3×10^{-7}	1.5×10^{-10}	2.5×10^{-9}
k_2	2.8×10^{-8}	2.2×10^{-10}	5×10^{-6}
k_{-2}	0	0	2×10^{-9}
k_3	2×10^{-10}	2.2×10^{-11}	0
$\partial\eta/\partial\log i$(V)†	0.075 to 0.125	0.125	~0.12
i_0(A cm^{-2})	3.1×10^{-4}	8.7×10^{-5}	3.1×10^{-4}
q_{max}(μC cm^{-2})	70	20	210
Mechanism	Discharge–parallel recombination–electrochemical desorption		Discharge–recombination

* Values quoted in Fig. 9 of [6]
† $b = (\partial\eta/\partial\log i)/2.303$

electrodes of Conway *et al.* [5], the η–log$i$ curves showed a constant slope of ~0.12 V in contrast to the dual slopes reported in [7].

Employing the kinetic rate constants in Table 1, the Tafel slope behaviour and the potential dependence of coverage was reexamined, using the generalized relationship for b, Equation 19, to understand the rationale for the two different mechanisms quoted in Table 1 for the HER on platinum in alkaline media at ~25° C. The Tafel slope and the coverage variations with potential, are depicted in Figs 3 and 4 along with the pseudocapacitance profiles in Fig. 5 using Equation 18, and the η–log$i$ plots in Fig. 6 for active and inactive platinum based on the discharge-parallel recombination–electrochemical desorption mechanism, hereafter termed D–PRE route and the discharge–recombination route using the k values in Table 1. The D–PRE mechanism shows θ–η variations on active platinum contributing to pseudocapacitance as observed experimentally in [5], where as with inactive platinum, which showed a b value of 120 mV, the pseudocapacitance was small, as it should be, since the rate of discharge is smaller by an order of magnitude compared to the rate of the recombination or the electrochemical desorption step. Surprisingly, however, the D–PRE route with the rate constants in Table 1 for active platinum exhibits a jump in the η–log$i$ curve (Fig. 6), calculated using Equation 12, where the Tafel slope value changes to 125 mV whereas the experimental curve shows a smooth transition during the change over of the slope from 75 to 125 mV. The rate constants for the D–PRE sequence for inactive platinum and the discharge–recombination path for platinum, on the other hand, shows η–log$i$ variations in agreement with the experimental observations up to an overpotential of 0.4 V, beyond which the discharge-recombination mechanism with the rate constants in Table 1 calls for the Tafel slope to go to infinity (see Fig. 6). The D–PRE mechanism, with the rate constants in Table 1, also predicts abnormal Tafel slope and reaction order dependence on potential for active platinum as shown in Fig. 7.

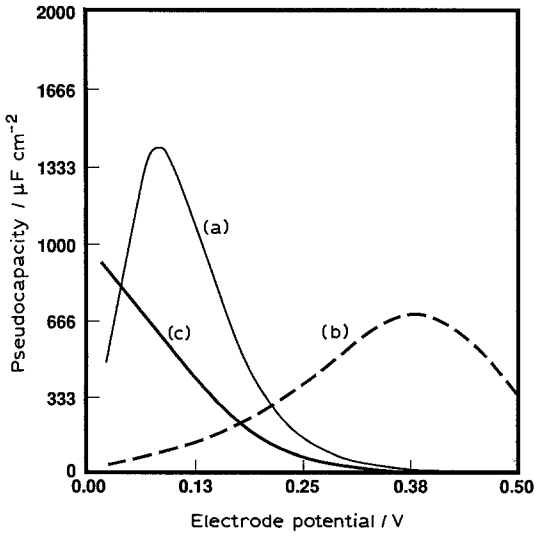

Fig. 5. Calculated pseudocapacitance variation with potential for the three cases cited in Fig. 3 and Table 1.

An alternate mechanistic pathway involving the discharge–electrochemical desorption mechanism (Equations 1 and 3) is now examined to describe the experimental observations outlined earlier. Tafel slope values calculated using $k_1 = 1 \times 10^{-8}$, $k_{-1} = 1 \times 10^{-7}$ and $k_3 = 8 \times 10^{-10}$ for active platinum [5, 7] were found to vary from ~$0.7RT/F$ in the low overpotential region to $2RT/F$ at overpotentials greater than 0.15 V. Similar Tafel slope behaviour was observed even when repulsive lateral interactions were considered in Equation 19; the potential dependence of coverage and pseudocapacitance being significant in the potential region where the Tafel slope is $< 2RT/F$ (see Figs 8 to 11). The discharge–electrochemical desorption mechanism, with the rate constants mentioned above, also predicts a normal pattern of variations of $\mathscr{R}$, b and θ with potential, shown in Fig. 12. The complex plane impedance plots (see Fig. 13), calculated using Equations 49 and 50a with $k_1 = 1 \times 10^{-8}$, $k_{-1} = 1 \times 10^{-7}$ and $k_3 = 8 \times 10^{-10}$ were also found to be in agreement with the experimental data schematically shown in Fig. 2. Inclusion

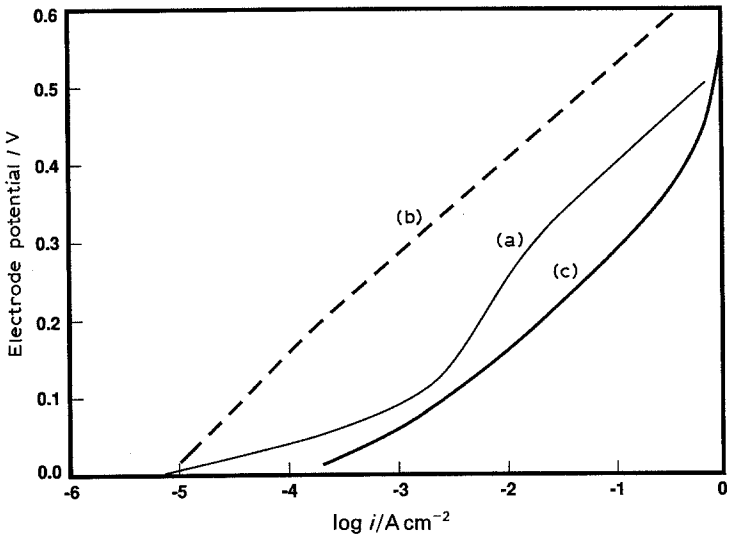

Fig. 6. Theoretical η–log$i$ variations for the three cases described in Fig. 3 and Table 1.

of g in Equation 49, instead of reduction in the magnitude of the saturation coverage [5], appears to accentuate the overlap of the two semicircles simulating the experimental observations, as noted previously [5].

The inactive platinum electrode exhibited an i_0 of 8.7×10^{-5} A cm^{-2} which may be compared to the corresponding value of 3.1×10^{-4} A cm^{-2} on active platinum, presumably as a result of the blockage of active sites by impurities leading to the retardation of the initial discharge step, following Conway *et al.* [5]. The variations of b, C_ϕ with η and the η–log$i$ curves were hence computed using $k_1 = 1 \times 10^{-8}$, $k_{-1} = 1 \times 10^{-7}$ and $k_3 = 8 \times 10^{-10}$ and illustrated in Figs 8 to 12. The corresponding a.c. impedance behaviour is illustrated in Fig. 14. These simulations with the *retarded* discharge rate for inactive platinum in Fig. 12 are in close agreement with the experimental observations.

Thus, the mechanism of HER in alkaline solutions appears to follow the discharge-slow electrochemical desorption pathway on active platinum, the discharge step being significantly slowed down on inactive platinum due to the blockage of the active sites.

4. Summary and conclusions

(i) A generalized procedure was developed to describe the Tafel slope and reaction order of electrochemical reactions involving several constituent steps.

(ii) Following the well accepted pathways for the HER, where the initial discharge step generating the adsorbed hydrogen intermediate is succeeded by the chemical or the electrochemical desorption of the chemisorbed H-species, global relationships for the Tafel slope, reaction order and the a.c. impedance were derived for the HER employing the steady-state approach. All the forward and backward rates of the component pathways were taken into consideration in these relationships along with possible lateral interactions between the adsorbed intermediates.

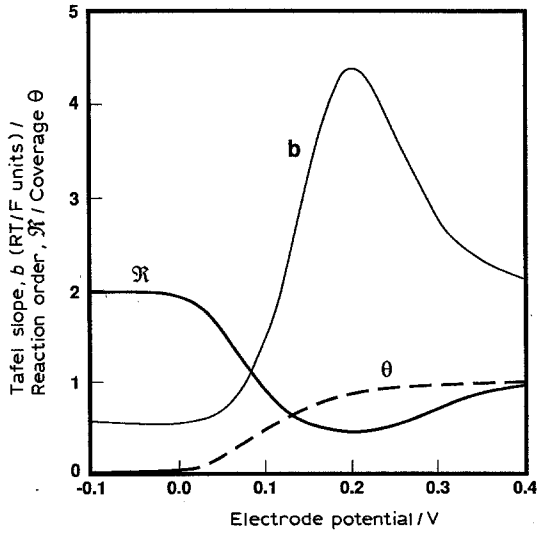

Fig. 7. Theoretical b, θ and $\mathscr{R}$ variations with potential expected of the behaviour of HER on active platinum in 0.5 M NaOH solutions for case a in Fig. 3.

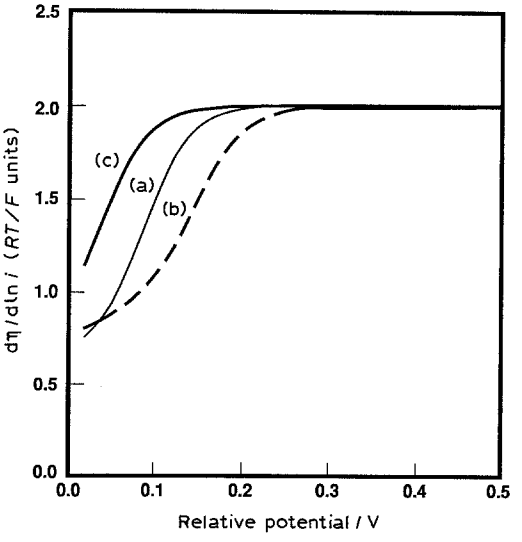

Fig. 8. Calculated Tafel slope variations with potential using the following rate constants: (a) $k_1 = 1 \times 10^{-8}$, $k_{-1} = 1 \times 10^{-7}$, $k_3 = 8 \times 10^{-10}$, $g = 0$; (b) $k_1 = 1 \times 10^{-8}$, $k_{-1} = 1 \times 10^{-7}$, $k_3 = 8 \times 10^{-10}$, $g = 10$; (c) $k_1 = 1 \times 10^{-10}$, $k_{-1} = 1 \times 10^{-9}$, $k_3 = 8 \times 10^{-10}$, $g = 0$.

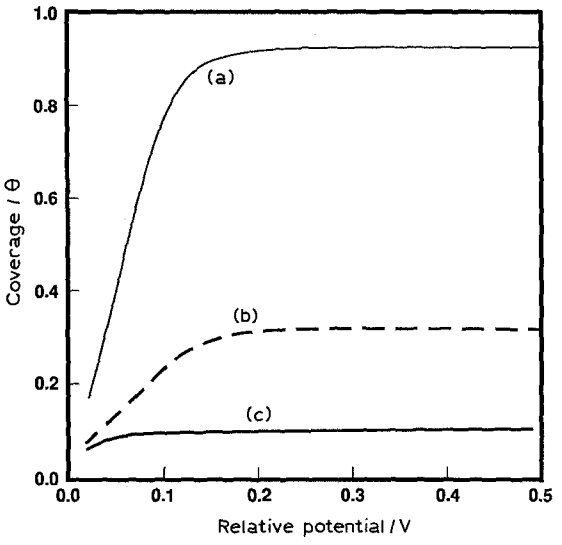

Fig. 9. Coverage variation with potential for the three cases described in Fig. 8.

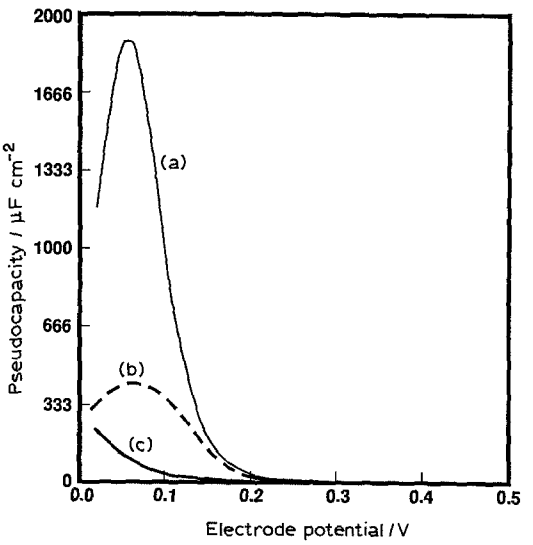

Fig. 10. Pseudocapacitance variation with potential for the three cases described in Fig. 8.

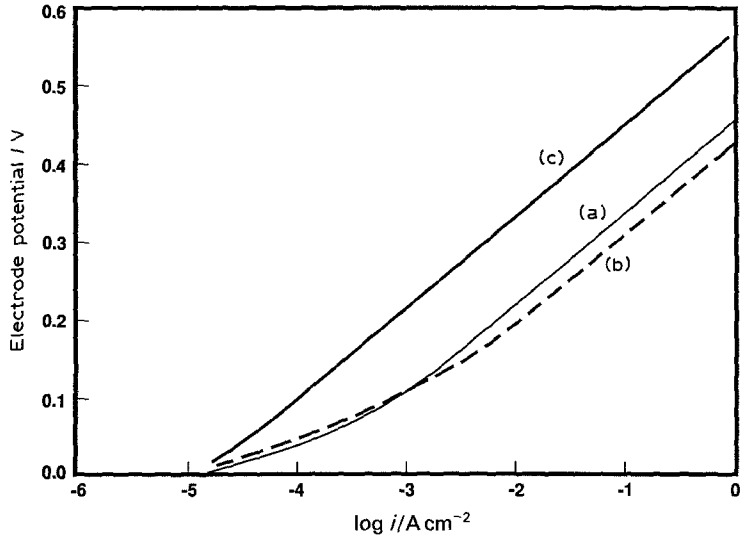

Fig. 11. Polarization curves calculated using the rate constants quoted in Fig. 8

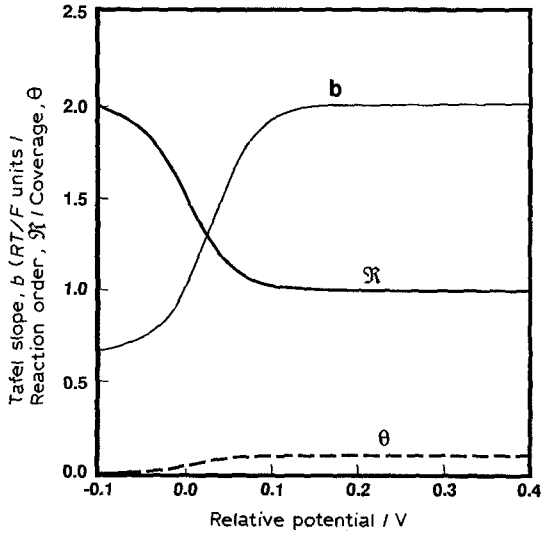

Fig. 12. Theoretical variation of Tafel slope, reaction order and coverage with potential using $k_1 = 1 \times 10^{-8}$, $k_{-1} = 1 \times 10^{-7}$, $k_3 = 8 \times 10^{-10}$ and $g = 0$.

(iii) Limiting relationships for the Tafel slope and reaction order, deduced from the general equation as special cases, are in agreement with those published previously.

(iv) Analysis of the kinetic data for the HER on platinum in alkaline media showed the cathodic hydrogen evolution reaction mechanism to follow the discharge-slow electrochemical desorption route, the discharge step being significantly retarded on inactive platinum due to blockage of active sites.

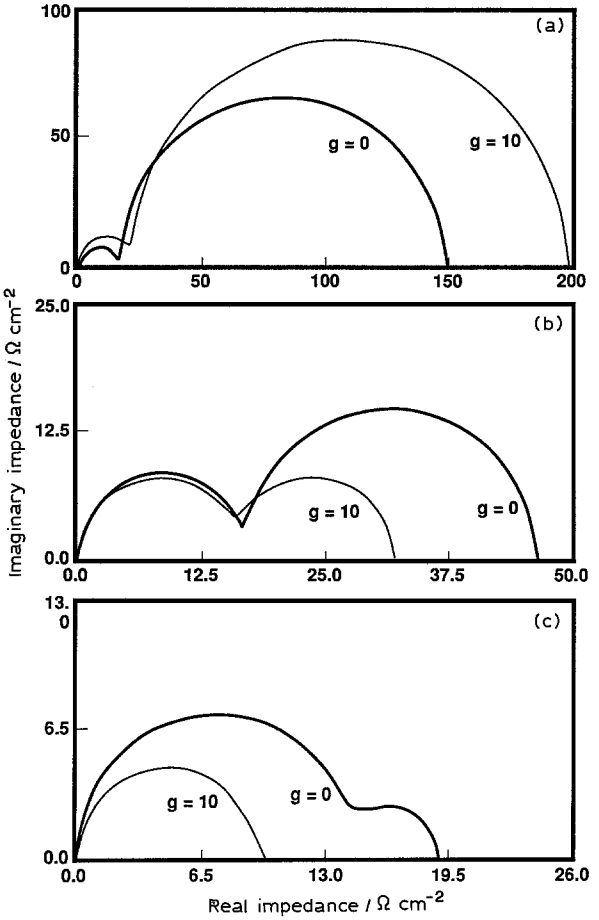

Fig. 13. Complex-plane diagrams computed using Equations 49 and 50 with the following rate constants for HER on active platinum in 0.5 M NaOH at various overpotentials for $g = 0$ and $g = 10$. $k_1 = 1 \times 10^{-8}$, $k_{-1} = 1 \times 10^{-7}$, $k_3 = 8 \times 10^{-10}$, $C_d = 25\,\mu F\,cm^{-2}$. Overpotential, η: (a) 0.05, (b) 0.10, and (c) 0.15 V.

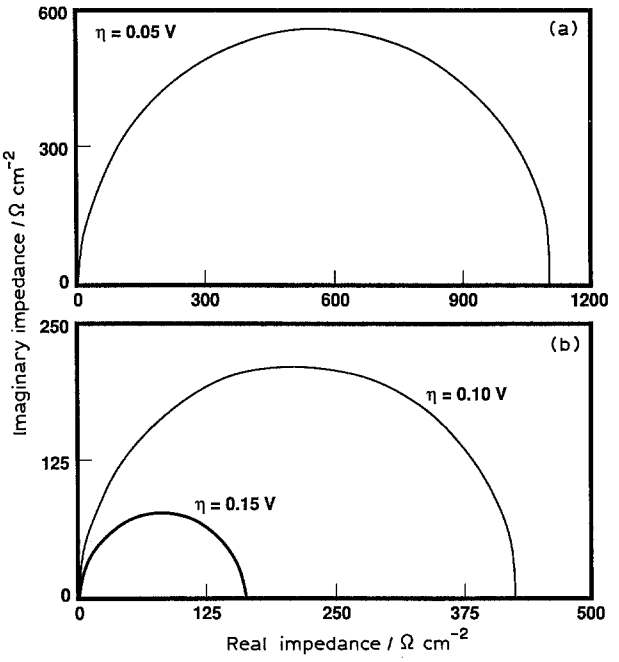

Fig. 14. Complex-plane diagrams computed using Equations 49 and 50a with $k_1 = 1 \times 10^{-10}$, $k_{-1} = 1 \times 10^{-9}$, $k_3 = 8 \times 10^{-10}$ for HER on inactive platinum in 0.5 M NaOH for $g = 0$, $C_d = 25\,\mu F\,cm^{-2}$ at (a) $\eta = 0.05$ V and (b) $\eta = 0.10$ V and 0.15 V.

References

[1] B. E. Conway, *in* 'Theory and Principles of Electrode Processes', Ronald Press, New York (1965) Chapter 8, p. 170.

[2] A. J. Appleby, H. Kita, M. Chemla and G. Bronoel, *in* 'Encyclopedia of Electrochemistry of the Elements', (edited by A. J. Bard), Marcel Dekker, New York (1982) Vol. XA, Chapter 3.

[3] J. O'. M. Bockris, *in* 'Modern Aspects of Electrochemistry', Butterworths, London (1954) Chapter 4.

[4] B. E. Conway and B. V. Tilak, *in* 'Advances in Catalysts', Vol. 38 (1992).

[5] L. Bai, D. A. Harrington and B. E. Conway, *Electrochim. Acta* **32** (1987) 1713.

[6] P. Ekdunge, K. Jüttner, G. Kreysa, T. Kessler, H. Ebert and W. J. Lorenz, *J. Electrochem. Soc.* **138** (1991) 2660.

[7] B. E. Conway and E. Gileadi, *Trans. Faraday Soc.* **58** (1962) 2493.

[8] B. V. Tilak and B. E. Conway, *Electrochim. Acta* **37** (1992) 51.

[9] B. V. Tilak, C.-P. Chen and B. E. Conway, *Electrochim. Acta*, in course of publication (1992).

[10] B. V. Tilak, C.-P. Chen and S. K. Rangarajan, *J. Electroanal. Chem.* **324** (1992) 405.

[11] B. E. Conway and L. Bai, *J. Electroanal. Chem.* **198** (1986) 149.

[12] B. E. Conway, L. Bai and D. F. Tessier, *J. Electroanal. Chem.* **161** (1984) 39.

[13] B. E. Conway and L. Bai, *J. Chem. Soc. Faraday Trans I* **81** (1985) 1841.